ELSEVIER

Journal of Alloys and Compounds 275–277 (1998) 398–401

Journal of ALLOYS AND COMPOUNDS

Simulation of the energy levels of Dy^{3+} in DyOCl

Jorma Hölsä[a], Ralf-Johan Lamminmäki[a,*], Pierre Porcher[b]

[a]*Department of Chemistry, University of Turku, FIN-20014 Turku, Finland*
[b]*CNRS, UPR 209, 1, Pl. A. Briand, F-92195 Meudon, France*

Abstract

The UV-vis-NIR absorption spectra of DyOCl were measured at selected temperatures between 9 and 300 K. The emission spectra of Dy^{3+} in LaOCl and GdOCl were obtained at 77 K and room temperature. The energy level scheme of Dy^{3+} was simulated with the aid of a phenomenological theory simultaneously taking into account both the free ion and crystal field (c.f.) effects. The model included 14 adjustable parameters describing the electrostatic and the configuration interaction as well as the spin-orbit coupling. The c.f. effect was accounted for by the five non-zero B_q^k parameters according to the C_{4v} point symmetry of Dy^{3+}. Good simulation of the experimental energy level scheme was achieved with a r.m.s. deviation of 21 cm^{-1} between the experimental and calculated energy level schemes of 179 Kramers doublets. A comparison to Pr^{3+} ($4f^2$), Nd^{3+} ($4f^3$), Sm^{3+} ($4f^5$), Eu^{3+} ($4f^6$), Tb^{3+} ($4f^8$), Ho^{3+} ($4f^{10}$), Er^{3+} ($4f^{11}$), and Tm^{3+} ($4f^{12}$ electron configuration) in other REOCl matrices showed smooth evolution of the free ion and c.f. effects. © 1998 Elsevier Science S.A.

Keywords: Dysprosium; Energy level simulation; Crystal field; Rare earth oxychlorides

1. Introduction

The rare earth oxyhalides, REOX (X=F, Cl, Br, and I), form a system where the change of both the cation and anion provides an opportunity to a systematic study of the changes in the electronic energy level schemes of the RE^{3+} ions. The lighter REOCl (RE=La–Er, and Y) as well as all oxybromides and oxyiodides have a Matlockite-type PbFCl structure which belongs to the tetragonal crystal system with P4/nmm (no. 129; $Z=2$) as the space group [1,2]. The RE^{3+} ion has C_{4v} point symmetry. The heavier oxychlorides beyond ErOCl [3] and most stoichiometric oxyfluorides crystallize with the hexagonal SmSI type structure [4].

Dy^{3+} has a $4f^9$ electron configuration which results in a complicated energy level scheme characterized by 198 *SLJ* manifolds which split in the presence of the crystal field (c.f.) interaction into a total of 1001 Stark levels in lower than cubic symmetry. The energy level scheme of Dy^{3+} has been simulated by using phenomenological models including the free ion and c.f. effects in DyOF [5], LaF_3 [6], $LaCl_3$ [7], DyODA [8], and DyDPA [9] hosts. A review on earlier works on Dy^{3+} and other rare earths has been published recently by Görller-Walrand and Binnemans [10].

In this work, the energy level scheme of the Dy^{3+} ion in DyOCl was deduced from the UV-vis-NIR absorption and visible luminescence spectra. The experimental scheme was simulated with a phenomenological model describing the electrostatic and interconfigurational interactions as well as the spin-orbit coupling taking simultaneously into account the c.f. effect, too. The free ion and c.f. parameters obtained were compared to those of the other RE oxychlorides ($RE^{3+}=Pr^{3+}$ [11], Nd^{3+} [12], Sm^{3+} [13], Eu^{3+} [14], Tb^{3+} [15], Ho^{3+} [13], Er^{3+} [16], and Tm^{3+} [17]) and the trends in the parameter values were discussed.

2. Experimental

The polycrystalline DyOCl sample was prepared by the solid state reaction between RE_2O_3 and NH_4Cl at 900°C for 1.5 h [18]. In order to avoid any remains of Dy_2O_3, a NH_4Cl/Dy_2O_3 ratio equal to 2.15 was used. For the luminescence measurements, the LaOCl and GdOCl hosts were doped with 1 mol.% of Dy^{3+}. The reaction temperature was 1000 and 900°C for LaOCl and GdOCl, respectively. All samples were checked by routine X-ray powder diffraction to ensure the purity of the samples. Also the

*Corresponding author. Tel.: +358 2 3336734; fax: +358 2 3336700; e-mail: ralflamm@utu.fi

PII: S0925-8388(98)00348-X

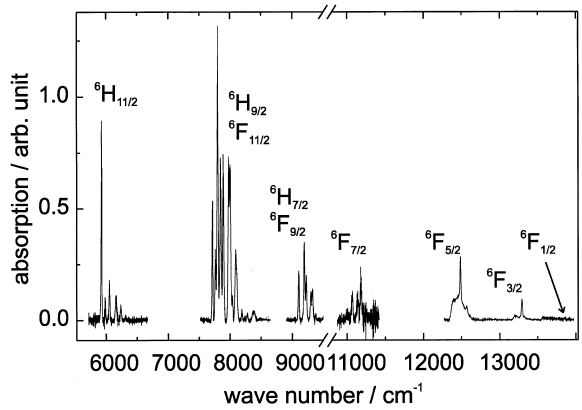

Fig. 1. Part of the absorption spectra of DyOCl at 9 K between 720 and 1750 nm (13 900–5700 cm^{-1}).

absence of additional lines in the optical spectra indicated that no impurity phases were present.

The luminescence spectra of the Dy^{3+}-doped LaOCl and GdOCl were recorded at 77 and 300 K in the visible region. The optical absorption spectra of DyOCl between 220 and 1750 nm were measured at selected temperatures between 9 and 300 K (Figs. 1 and 2). The techniques have been described in detail in earlier works [11–17].

3. Results and discussion

3.1. Analysis of the optical spectra

The number of the Stark levels for a particular free ion $^{2S+1}L_J$ state is $J+1/2$ for lower than cubic symmetries as C_{4v} for Dy^{3+} in DyOCl [19]. There are only two types of Stark levels corresponding to the irreducible representations $D_{1/2}$ and the Kramers conjugate state ($_2S$). According to the group theoretical selection rules, the transitions between all c.f. levels are allowed as both e.d. and m.d. transitions [19].

The visible emission of the Dy^{3+} ion originating from

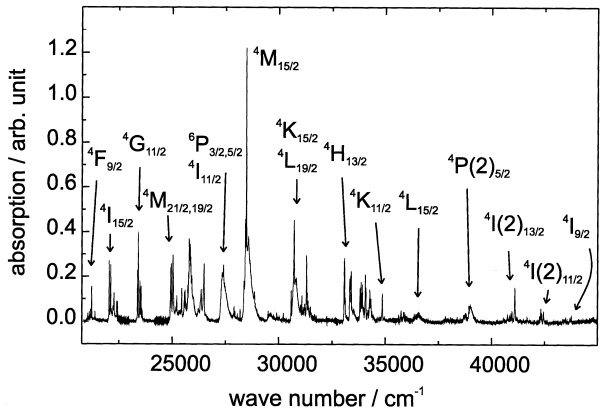

Fig. 2. Part of the absorption spectra of DyOCl at 9 K between 222 and 465 nm (45 000–21 500 cm^{-1}). Not all of the states are marked.

the transition from the $^4F_{9/2}$ to $^6H_{13/2}$ was recorded for the LaOCl and GdOCl matrices between 544 and 590 nm. The emission to the $^6H_{15/2}$ ground state could not be observed because the $^4F_{9/2}\rightarrow{}^6H_{15/2}$ transition energy was too close to the Ar^+ excitation line at 457.9 nm. Not all components of the $^6H_{13/2}$ state were observed since only five out of seven were found for the GdOCl matrix and even less for LaOCl. The energy levels observed in the GdOCl matrix were used in the calculations to minimise the effect of the ionic radius difference between the Dy^{3+} ion and the host cation.

The optical absorption of Dy^{3+} in DyOCl was measured at selected temperatures between 9 and 300 K in order to find out the splitting of the $^6H_{15/2}$ ground state, inaccessible by the luminescence measurements. From the hot band absorption, five Stark levels of the ground state (0, 12, 240, 325 and 380 cm^{-1}) could be resolved. Low temperatures facilitated also the separatation of the transitions from the two lowest Stark levels and to avoid the temperature broadening of the lines.

In the NIR area, the first state observed by absorption was $^6H_{11/2}$, from which five Stark levels out of six were observed between 1600 and 1700 nm. Also regions from 1200 to 1300 and from 1060 to 1100 nm were well observed, but the $^6H_{9/2}$ and $^6F_{11/2}$, as well as the $^6H_{7/2}$ and $^6F_{9/2}$ states, partially overlap, respectively. A total of 15 out of the 20 Stark levels were found. The $^6H_{15/2}\rightarrow{}^6F_{7/2}$ transition between 890 to 910 nm was only weakly observed due to the weak detection in that region. Still, three out of the four Stark levels were obtained. Absorption to the $^6H_{5/2}$ state was not observed. The $^6H_{15/2}\rightarrow{}^6F_{5/2}$, $^6F_{3/2}$, $^6F_{1/2}$ transitions were observed from 720 to 810 nm. The transition to the $^6F_{1/2}$ state is forbidden due to the $\Delta J\leq 6$ free ion selection rule [20] but was observed anyhow due to the lifting of this selection rule by the c.f. effect.

In the UV-vis region absorption to the first three states ($^4F_{9/2}$, $^4I3_{15/2}$, and $^4G4_{11/2}$) were well separated and a total of 17 out of 19 Stark levels were observed. Beyond 400 nm, in Fig. 2, 25 000 cm^{-1} the density and wave function mixing of the J states becomes high resulting in severe overlap and difficult assignment of the different J states. The last Stark levels, owing to absorption to the $^2K5_{13/2}$ state, were observed at 228 nm. The number of the Stark levels observed from absorption spectra was 174 which represents 56 SLJ manifolds including the $^4D3_{7/2}$, $^6F_{1/2-11/2}$, $^4F2_{5/2-9/2}$, $^4F3_{3/2-9/2}$, $^4G2_{5/2-11/2}$, $^4G4_{9/2-11/2}$, $^6H_{7/2-11/2,15/2}$, $^4H1_{7/2-13/2}$, $^4I2_{9/2-15/2}$, $^4I3_{9/2-15/2}$, $^4K1_{11/2-17/2}$, $^2K5_{13/2}$, $^4L_{13/2-19/2}$, $^2L3_{15/2,17/2}$, $^4M_{17/2-21/2}$, $^2N_{21/2}$, $^6P_{3/2-7/2}$, and $^4P2_{3/2,5/2}$ states.

3.2. Simulation of the energy level scheme

The energy level structure of the RE^{3+} ions is created by different interactions which are usually separated into

two parts: first, those due to the intraionic effects, i.e. the free ion interactions, and second, to the external effects represented by the crystal field arising from the influence of the surrounding charges on the 4f electrons of the RE^{3+} ion in the solid state. The effect of these interactions on the energy level scheme of the RE^{3+} ion can be characterized with a combined energy Hamiltonian H_{TOT}, which includes one or several parameters for each interaction [20,21]:

$$H_{TOT} = H_0 + \sum_{k=0,1}^{2,3} E_k(\mathrm{nf,nf})\, e^k + \zeta_{4f} A_{SO} + \alpha L(L+1) + \beta G(G_2) + \gamma G(R_7) + \sum_{k=2,3,4}^{6,7,8} T^k t_k + \sum_{k,q,i} B_q^k C_q^k(i)$$

In this expression the free ion part consists of a spherically symmetric, one-electron term H_0 which is the same for the whole $4f^N$ configuration. The Racah parameters E_k and the spin-orbit coupling constant ζ_{4f} describe the electrostatic interaction between the 4f electrons and the coupling of the electron spin and orbital momentum, respectively. The Trees parameters α, β, γ and Judd parameters T^k accounting for the two- and three-body terms for the configuration interactions [21], respectively, induce only minor effects to the energy level scheme. The terms accompanying the parameters denote the corresponding effective operators.

In the one-electron c.f. part of the total Hamiltonian, C_q^k are related to the spherical tensors of rank k, dependent on the coordinates of the ith electron with summation over all 4f electrons. B_q^k are the real c.f. parameters, the number of which is defined by the site symmetry of the RE^{3+} ion [19]. For the rather high C_{4v} symmetry of the Dy^{3+} site in DyOCl, the number of the non-zero c.f. parameters is restricted to five, i.e. B_0^2, B_0^4, B_4^4, B_0^6 and B_4^6.

As the starting values for the free ion parameters those of the DyOF system were used [5]. The initial c.f. parameter values were interpolated from earlier calculations for the other REOCl:RE^{3+} systems [13]. The simulation method used varies simultaneously both the free ion and c.f. parameters using a non-truncated set of wavefunctions. The best fit set of parameters was obtained by the least-squares refinement between the observed and calculated energy level values through minimising the r.m.s. function σ [22].

179 Stark levels out of 1001 levels were derived from the absorption and luminescence spectra. A set of 19 parameters including 14 free ion and five c.f. parameters were used in the final simulation of the energy level scheme. The degrees of freedom are high enough to allow a reliable variation of all parameters involved.

In the beginning of the simulation only the most isolated free ion states were utilised. The calculations were carried out with a step by step variation of the different parameters, i.e. first only the Racah parameters E_k were varied, after which the spin-orbit coupling constant ζ_{4f} and next the two-body interaction parameters were released to vary. The c.f. parameters were varied before the Judd parameters because of the uncertainty of the latter. In each step the r.m.s. function was minimised before the next parameters were allowed to vary. After achieving constant values for the parameters more Stark levels were added and the simulation procedure was repeated. The calculations resulted in the following free ion and c.f. parameter set (with the estimated standard deviations): E_0, 55082(1); E_1, 6100.9(3); E_2, 30.14(1); E_3, 613.92 (5); α, 17.63(2); β, −642(2); γ, 1851(2); ζ_{4f}, 1916.5(8); T^2, 313(1); T^3, 42(4); T^4, 75(8); T^6, −345(10); T^7, 330(8); T^8, 346(5); B_0^2, −984(14); B_0^4, −711(30); B_4^4, ±988(22); B_0^6, 657(31); and B_4^6, ±158(34). The energy level scheme of the Dy^{3+} ion was well simulated as a whole. A good agreement between the observed and calculated level values was achieved with the rms deviation of 21 cm^{-1}.

3.3. Evolution of the free ion and c.f. interactions

The free ion parameters for the RE^{3+} (Pr^{3+}, Nd^{3+}, Sm^{3+}, Eu^{3+}, Tb^{3+}, Dy^{3+}, Ho^{3+}, Er^{3+}, and Tm^{3+}) series show an increase in the electrostatic interaction (the Racah parameters) and in the spin-orbit coupling towards the heavier RE^{3+} ions (Fig. 3) because of the increasing repulsion experienced by the 4f electrons. The trends in the configuration interaction terms α, β, and γ (Fig. 3) are less clear, although regular, probably as they have a less important contribution to the $4f^N$ energy level scheme. The Judd T^k parameters describing the three-body configuration interactions were, in some cases [13,16], fixed close to conventional values, because the parameter values have a strong dependence on certain levels only.

The evolution of the c.f. parameter values for the REOCl or GdOCl matrices as a function of the number of the 4f electrons (N) is rather smooth (Fig. 4). Due to the increased nuclear charge experienced by the electrons with increasing N, the B_q^k values are expected to decrease. This trend seems to hold up to the middle of the series after which the c.f. effect regains some strength as shown by the second- and fourth-rank parameters. One explanation for

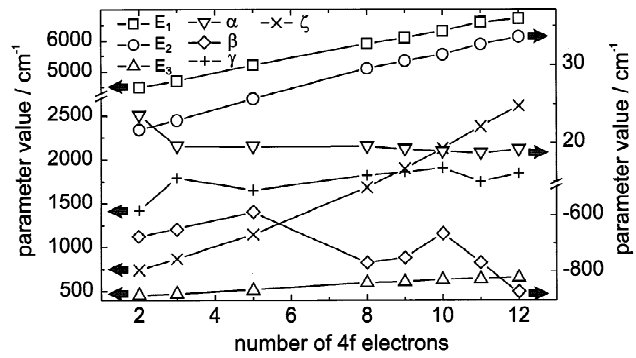

Fig. 3. The evolution of the free ion parameters in the REOCl (or GdOCl:RE^{3+}) series [11–17].

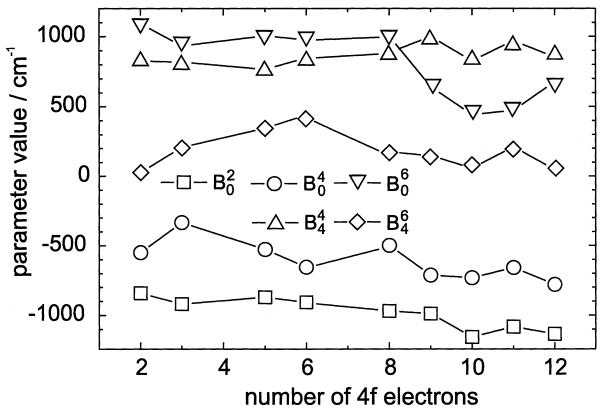

Fig. 4. The evolution of the c.f. parameters in the REOCl (or GdOCl:RE^{3+}) series [11–17].

this might be the possible inadequacy of the one-electron c.f. operator to describe the c.f. interaction of the heavier rare earths. Also, beyond the middle of the RE^{3+} series, other factors, e.g. the energy of the 5s (and 5d) orbitals may have additional influence on the c.f. parameter values. In principle, the lowering of the 5s (and 5d) orbital energy should strengthen the c.f. effect by increasing the mixing of the opposite parity terms to the 4f wave functions. The doping of the heavier RE^{3+} ions in the GdOCl matrix may also have some additional influence to the observed trends due to the local structural distortion observed by the RE^{3+} ion.

Further work is in progress in order to reduce the possible inadequacies due to the use of the basic parametrization scheme alone, for example the inclusion of the Marvin integrals (P^k and M^k) is to be made. The study of the REOBr series, which has the advantage of having the same tetragonal structure as that of the REOCl series, can also yield additional information on the trends involved in the REOCl series.

4. Conclusions

A total of 179 c.f. components representing 57 *SLJ* states of the Dy^{3+} ion were resolved from the analyses of the optical spectra of DyOCl. The energy level scheme of the Dy^{3+} ion in DyOCl was successfully simulated according to the C_{4v} site symmetry by a phenomenological model using 14 free ion and five c.f. parameters with a r.m.s. deviation of 21 cm^{-1}. The results for DyOCl were found consistent with those for other RE^{3+} (Pr^{3+}, Nd^{3+}, Sm^{3+}, Eu^{3+}, Tb^{3+}, Dy^{3+}, Ho^{3+}, Er^{3+}, and Tm^{3+}). The increase in the free ion parameter values from Pr^{3+} to Tm^{3+} indicates increasing electrostatic repulsion and spin-orbit coupling between the 4f electrons. In the entire REOCl:RE^{3+} series [13], the c.f. parameters evolve quite smoothly. However, some irregularities exist and possible explanations include: the structural distortion of the GdOCl lattice caused by the doping by other RE^{3+} ions, the possible inadequacy of the one-electron c.f. operator to describe the c.f. interaction for the heavier rare earths, the change of the energy of the 5s (and 5d) orbitals, and the inadequacies in the basic free ion parametrization scheme.

References

[1] L.G. Sillén, A.-L. Nylander, Svensk Kem. Tidskr. 53 (1941) 367.
[2] I. Mayer, S. Zolotov, F. Kassierer, Inorg. Chem. 4 (1965) 1637.
[3] H.P. Beck, Z. Naturforsch. 316 (1976) 1562.
[4] W.H. Zachariasen, Acta Crystallogr. 4 (1951) 231.
[5] J. Hölsä, E. Kestilä, R. Saez-Puche, P. Dereń, W. Stręk, P. Porcher, J. Phys. Condens. Matter 8 (1996) 1575.
[6] W.T. Carnall, G.L. Goodman, K. Rajnak, R.S. Rana, J. Chem. Phys. 90 (1989) 3443.
[7] C.K. Jayasankar, F.S. Richardson, M.F. Reid, J. Less-Common Metals 148 (1989) 289.
[8] D.H. Metcalf, T.A. Hopkins, F.S. Richardson, Inorg. Chem. 34 (1995) 4868.
[9] T.A. Hopkins, D.H. Metcalf, F.S. Richardson, Inorg. Chem. 34 (1995) 4879.
[10] C. Görller-Walrand, K. Binnemans, Rationalization of crystal-field parametrization, in: K.A. Gschneider Jr., L. Eyring (Eds.), Handbook Phys. Chem. Rare Earths, ch. 155, Elsevier, Amsterdam, 1996, pp. 139–141.
[11] E. Antic-Fidancev, J. Hölsä, M. Lemaître-Blaise, P. Porcher, J. Chem. Soc.: Faraday Trans. 87 (1991) 3625.
[12] L. Beaury, Ph.D. Thesis, Université de Paris-Sud, Orsay France, 1988, p. 128.
[13] J. Hölsä, R.-J. Lamminmäki, J. Lumin. 69 (1996) 311.
[14] J. Hölsä, P. Porcher, J. Chem. Phys. 75 (1981) 2108.
[15] J. Hölsä, R.-J. Lamminmäki, P. Porcher, H.F. Brito, Quim. Nova 19 (1996) 237.
[16] J. Hölsä, E. Säilynoja, R.-J. Lamminmäki, P. Dereń, W. Stręk, P. Porcher, J. Chem. Soc.: Faraday Trans. 93 (1997) 2241.
[17] J. Hölsä, R.-J. Lamminmäki, P. Porcher, J. Phys.: Condens. Matter 7 (1995) 5127.
[18] J. Hölsä, L. Niinistö, Thermochim. Acta 37 (1980) 155.
[19] J.L. Prather, NBS Monograph (US), 19 (1961) pp. 19 and 58.
[20] B.G. Wybourne, Spectroscopic Properties of Rare Earths, ch. 6, Interscience, New York, 1965.
[21] H. Crosswhite, H.M. Crosswhite, B.R. Judd, Phys. Rev. 169 (1979) 11.
[22] P. Porcher, Computer programs REEL and IMAGE for the simulation of d^N and f^N configurations involving the real and complex crystal field parameters, 1989, unpublished data.